Solar Flares and Magnetospheric Particles. Investigations Based Upon the ONR-602 and ONR-604 Experiments

AD-A273 639

Performance Report

DTIC
ELECTE
DEC 13 1993
S A

ONR Grant

N00014-90-J-1466

Fourth Quarter FY93

John P. Wefel and T. Gregory Guzik

Department of Physics and Astronomy
Louisiana State University
Baton Rouge, LA 70803-4001

Phone: 504-388-8696
FAX: 504-388-1222

This document has been approved for public release and sale; its distribution is unlimited.

30 November 1993

93-31326

93 12 10 031

"Solar Flares and Magnetospheric Particles: Investigations Based Upon the ONR-602 and ONR-604 Experiments"

I. Introduction:

This performance report covers work accomplished under ONR Grant N00014-90-J-1466 related to the radiation environment in near-Earth space. The goal of the research is to measure and describe, quantitatively, the Geospace radiation environment in which men and spacecraft must survive and function. The tools for this investigation are the data returned by the ONR-602 and ONR-604 experiments, both flown under the auspices of ONR and the Air Force Space Test Program, augmented by correlative databases of both space-based and ground-based data. The investigation involves data analysis, modeling and applications to a variety of space equipment and environments.

This report builds upon the detailed Technical Report (Fall, 1992) and the previous performance reports. For the current period, the principal effort was in the modeling of the Anomalous Component, determining the modulation level during the CRRES Mission, and studying the quiet-time particle access to the magnetosphere.

II. The Anomalous Component:

As described in the previous report, it is necessary to have a representation of the Anomalous Component (AC), particularly the anomalous helium in order to understand the solar modulation level as a function of time. Therefore, we have undertaken the task to develop realistic local interstellar spectra (LIS) for the anomalous cosmic rays.

An anomalous component to the observed cosmic ray spectrum has been reported for the elements helium, carbon, nitrogen, oxygen, neon, and argon. All six of these elements have high first ionization potentials and are present in the interstellar medium as neutral atomic matter. Anomalous component cosmic rays are widely believed to originate as neutral atoms in interstellar space, which drift into the inner solar system and are subsequently photoionized by solar UV radiation and swept back outward by the solar wind. Since the AC species are ionized by solar UV, one expects the AC cosmic rays to be singly charged.

Acceleration at the shock boundary of the heliosphere produces a local "interstellar" spectrum, which is then modulated in the heliosphere as the energetic particles move back toward Earth. The energies consistent with acceleration at the heliospheric shock boundary are low, and the AC local interstellar spectra are consequently very steep, essentially vanishing at energies above about 1 GeV per nucleon. The low energy of the AC cosmic rays accounts for their near absence from measured cosmic ray fluxes during periods of high solar modulation. However, the AC contribution at low energies has been observed in both the mid-70's and the mid-80's, during successive minima in the solar cycle, and is expected to return during each solar minimum period.

For our present work, it was decided to develop AC local interstellar spectra only for helium, nitrogen, oxygen, and neon. The observed AC fluxes for carbon and especially argon are quite low, and the inclusion of anomalous components of these species would not significant. The AC contribution is more significant for the remaining four elements, and in particular, it is important to include the AC helium in the analysis of the solar modulation level as a function of time, as described in the next section. For each of the four elements included, the model AC spectrum contains only the primary isotope (i.e., ^{4}He, ^{14}N, ^{16}O, and ^{20}Ne). Contributions from other

DTIC QUALITY INSPECTED 3

Codes

Dist | Avail and / or Special

A-1

isotopes would be very small compared to the primary isotope, and considering that the AC flux itself is comparatively small except at the lowest energies, the added refinement of attempting to model the isotopic composition is not warranted at this stage.

The helium and oxygen local interstellar spectra were derived at the University of Chicago, by demodulation of measured data (Garcia-Munoz, private communication) and have been adopted for this analysis. The LIS for nitrogen and neon were obtained by renormalizing the oxygen spectrum, with the normalization factor chosen to yield the best fit obtainable to a variety of measured AC datasets corresponding to different levels of modulation and different locations in the heliosphere. It was possible to obtain reasonable fits to the datasets for these three elements at energies above about 10 MeV/nucleon using just a single spectral shape, that of the demodulated oxygen spectrum. Measurements from IMP-8 at 1 AU, the Voyager spacecraft at 2 and at 21 AU, and Pioneer 10 at 16 AU were used in fitting the AC spectra. Details of these fits are summarized in Table 1.

Figure 1 shows the Local Interstellar Spectra (LIS) that have been adopted for the four anomalous elements that have been studied. The LIS are cut-off at 5 MeV/nucleon, but the N, O and Ne would be expected to turn-over, like the He, at lower energies. Modeling this turnover has not been possible within the available data. Figures 2-9 show the results of our predictions, using the spectra of Figure 1 as input, compared to the measurements cited in Table 1. The LIS were modulated to the time interval and the location in the heliosphere of the spacecraft from which the data were reported. The agreement between the predictions (solid lines) and the data points is reasonably good except for Voyager II results from 1985-86 at 21 AU for N and O below 10 MeV/nucleon. The equivalent data for anomalous Ne, however, is in good agreement with the predictions. Whether this indicates a problem with the N and O data during 1985-86 or with the predictions is unknown. The agreement for E>10 MeV/nucleon is, however, good enough for the purposes of the present study.

Note that the AC is singly charged and has, therefore, a higher rigidity than a Galactic Cosmic Ray (GCR) ion of the same energy. In order to combine the AC spectra with the GCR spectra, a routine was written to generate a binary file that mimics the output of the GCR propagation calculation. The solar modulation program accepts this file, modulates the elements with a charge of +1, then outputs the spectra on the same energy grid as the GCR spectra. The modulated AC spectra can then be added point-by-point to the GCR spectra, if desired. It is important to note that the AC must be modulated separately from the GCR component, because of its singly-charged ionization state.

During the CRRES period, the highest level of modulation occurred at the beginning of the mission. Taking the period from 8/19 - 12/15/90, the mean modulation level is characterized by value of ϕ = 1589 MV. Figure 10 shows spectra for He, N, O, and Ne modulated to this level. The solid curve includes the AC while the dashed curve does not. As expected from previous measurements, there is essentially no AC helium present. A surprise, however, is the N, O and Ne which each show a small amount of AC just above 10 MeV/nucleon even at these high levels of modulation. The explanation, we believe, is that, being singly-charged, the rigidity for N, O and Ne is so much larger than for He that the modulation cannot stop some penetration of these ions to 1 AU even at solar maximum! Understanding this effect quantitatively will require additional analysis (unfortunately ONR-604 cannot check the result because it is not sensitive at these low energies), but this may also help to explain the source of the "trapped anomalous oxygen" reported recently from measurements on the SAMPEX spacecraft (Cummings et al., GRL, 20, 2003, 1993).

Table 1. Details of anomalous component data fits

Anomalous species:	Helium
Spectrum:	Demodulated at University of Chicago
Fits:	See reference
Reference:	Garcia-Munoz, et al. 21st ICRC, 6, 164, 1990
Anomalous species:	Oxygen
Spectrum:	Demodulated at University of Chicago
Fits:	IMP-8, 1 AU, 1977, Phi = 506 MV Voyager I & II, 2 AU, 9/77 - 2/78, Phi = 513 MV Pioneer 10, 15 AU, 1/77 - 3/78, Phi = 513 MV Voyager II, 21 AU, 10/85 - 8/86, Phi = 693 MV
Reference:	Garcia-Munoz, et al., unpublished figure Cummings, Stone, and Webber, Ap J, 287, L99 - L103, 15 Dec. 1984 Cummings and Stone, Solar Wind VI Proc., NCAR/TN - 306+ PROC, V. J. Pizzo, Ed., 1988
Anomalous Species:	Nitrogen
Spectrum:	Normalized point-by-point from anomalous oxygen spectrum: Nitrogen flux = (Oxygen flux)/4.502
Fits:	Voyager I & II, 2 AU, 9/77 - 2/78, Phi = 513 MV Voyager II, 21 AU, 10/85 - 8/86, Phi = 693 MV
Reference:	Cummings, Stone, and Webber, Ap J, 287, L99 - L103, 15 Dec. 1984 Cummings and Stone, Solar Wind VI Proc., NCAR/TN - 306+ PROC, V. J. Pizzo, Ed., 1988
Anomalous species:	Neon
Spectrum:	Normalized point-by-point from anomalous oxygen spectrum: Neon flux = (Oxygen flux)/47.147
Fits:	Voyager I & II, 2 AU, 9/77 - 2/78, Phi = 513 MV Voyager II, 21 AU, 10/85 - 8/86, Phi = 693 MV
Reference:	Cummings, Stone, and Webber, Ap J, 287, L99 - L103, 15 Dec. 1984 Cummings and Stone, Solar Wind VI Proc., NCAR/TN - 306+ PROC, V. J. Pizzo, Ed., 1988

Fig. 1. Anomalous Local Interstellar Spectra

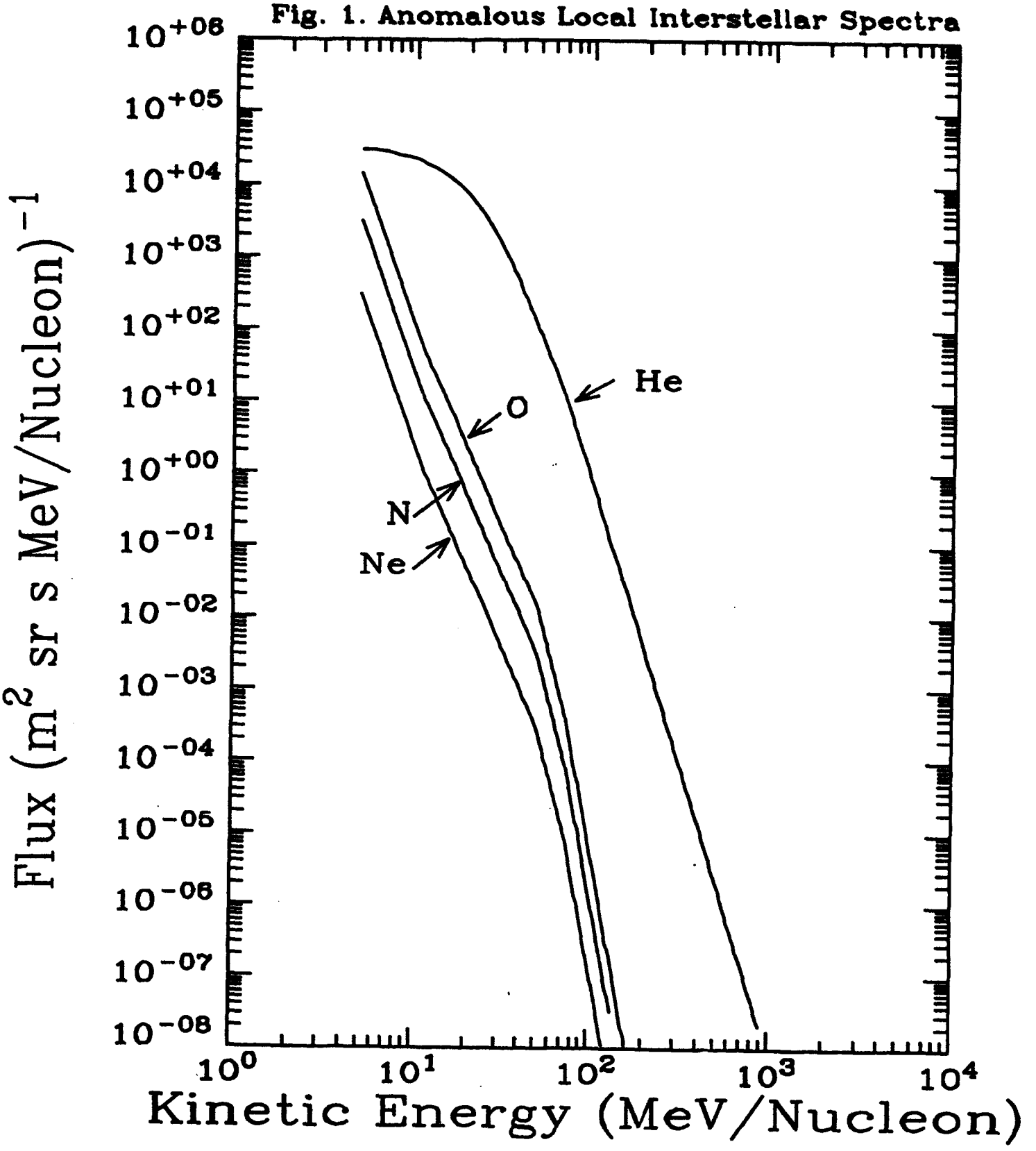

Fig. 2. Anomalous Oxygen at 1 AU

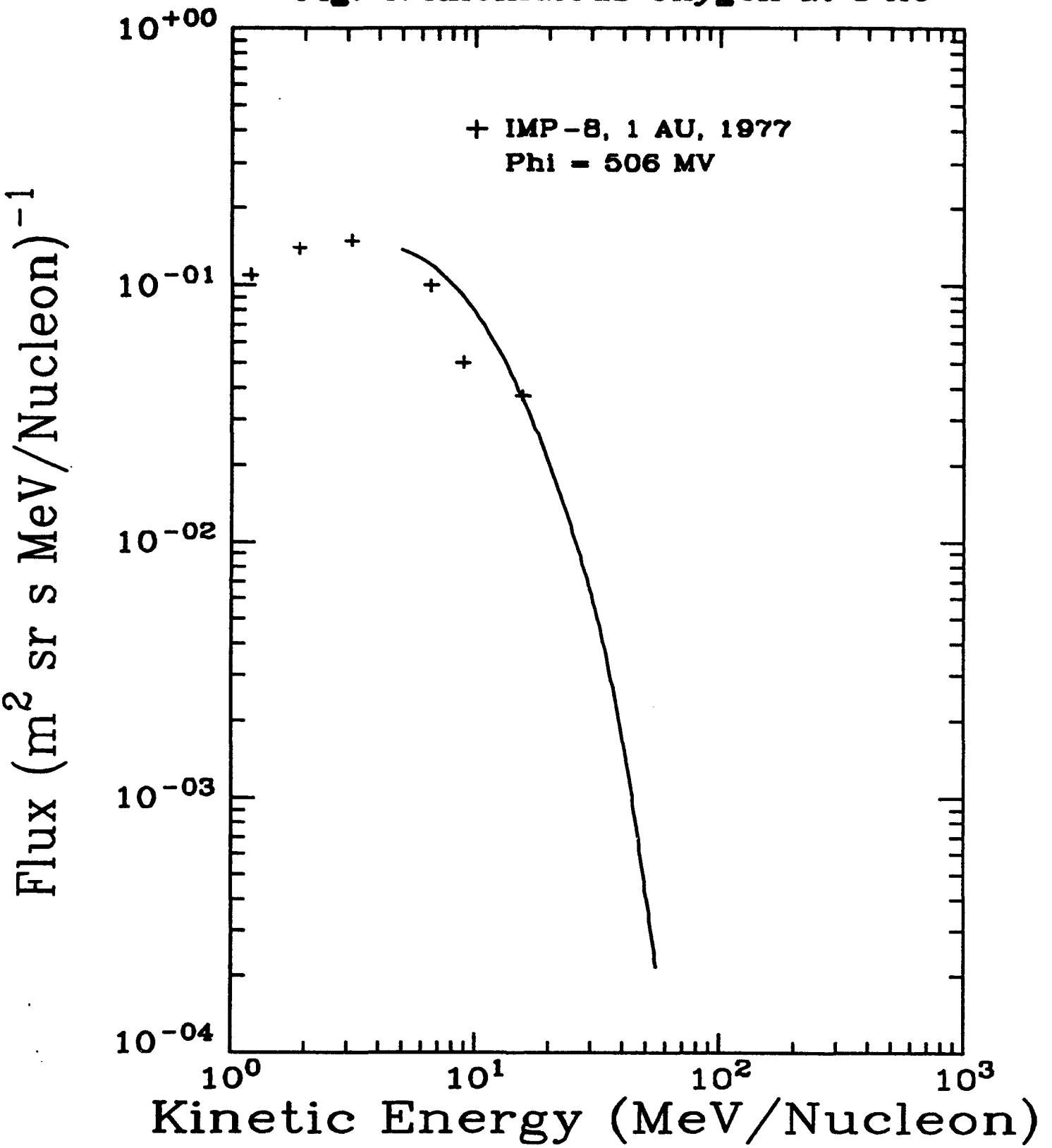

Fig. 3. Anomalous Oxygen at 2 AU

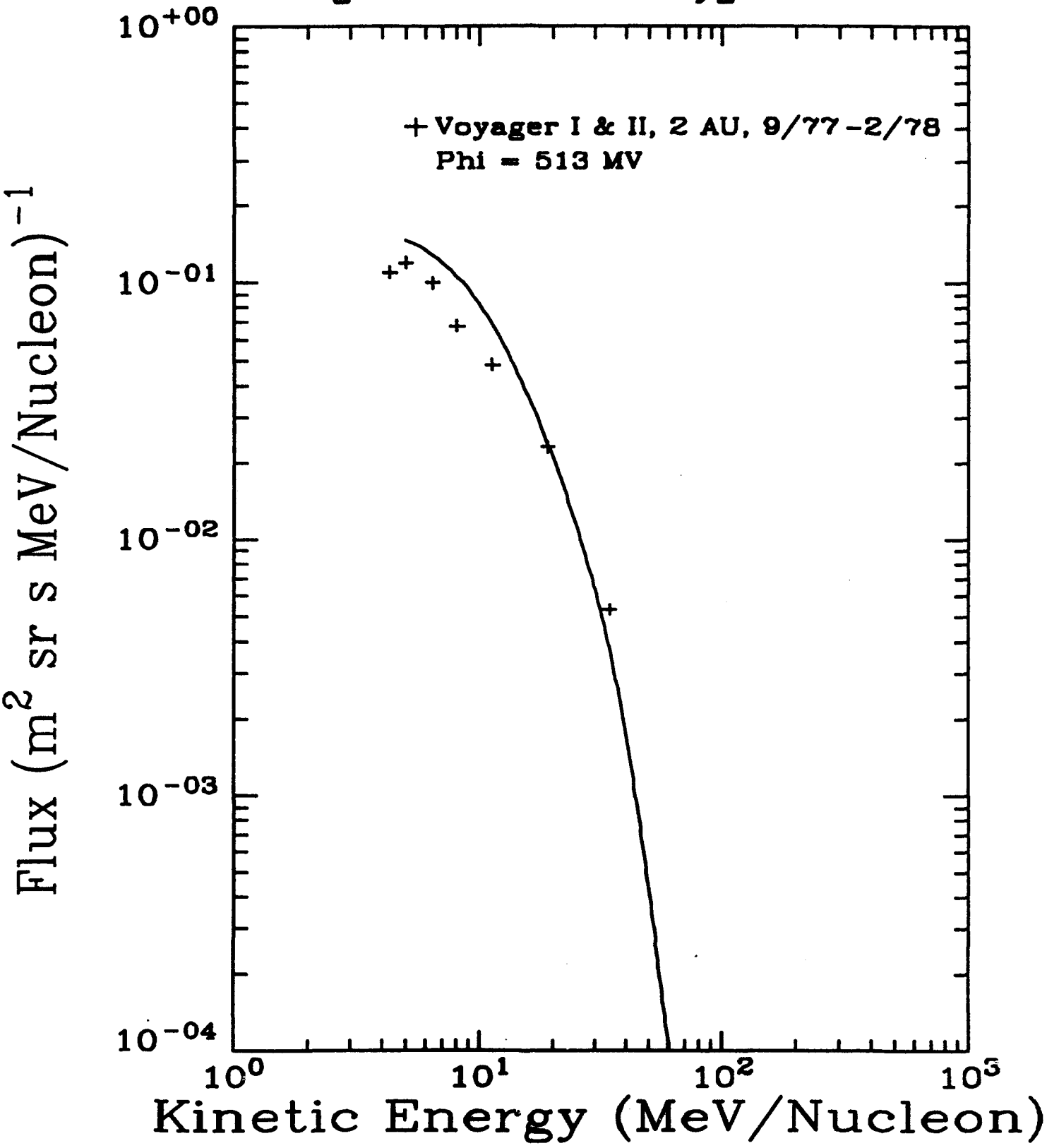

Fig. 4. Anomalous Oxygen at 15 AU

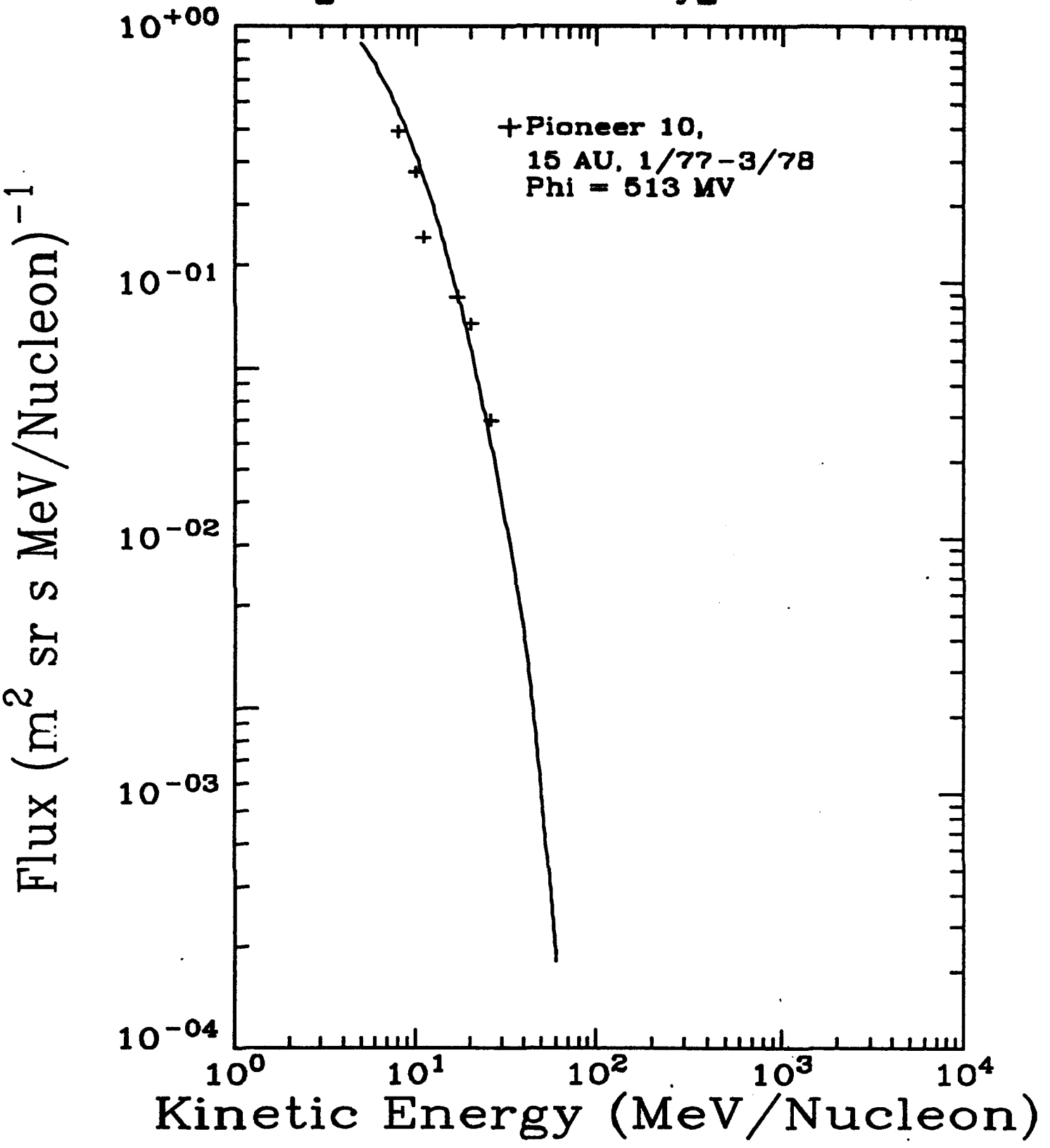

Fig. 5. Anomalous Oxygen at 21 AU

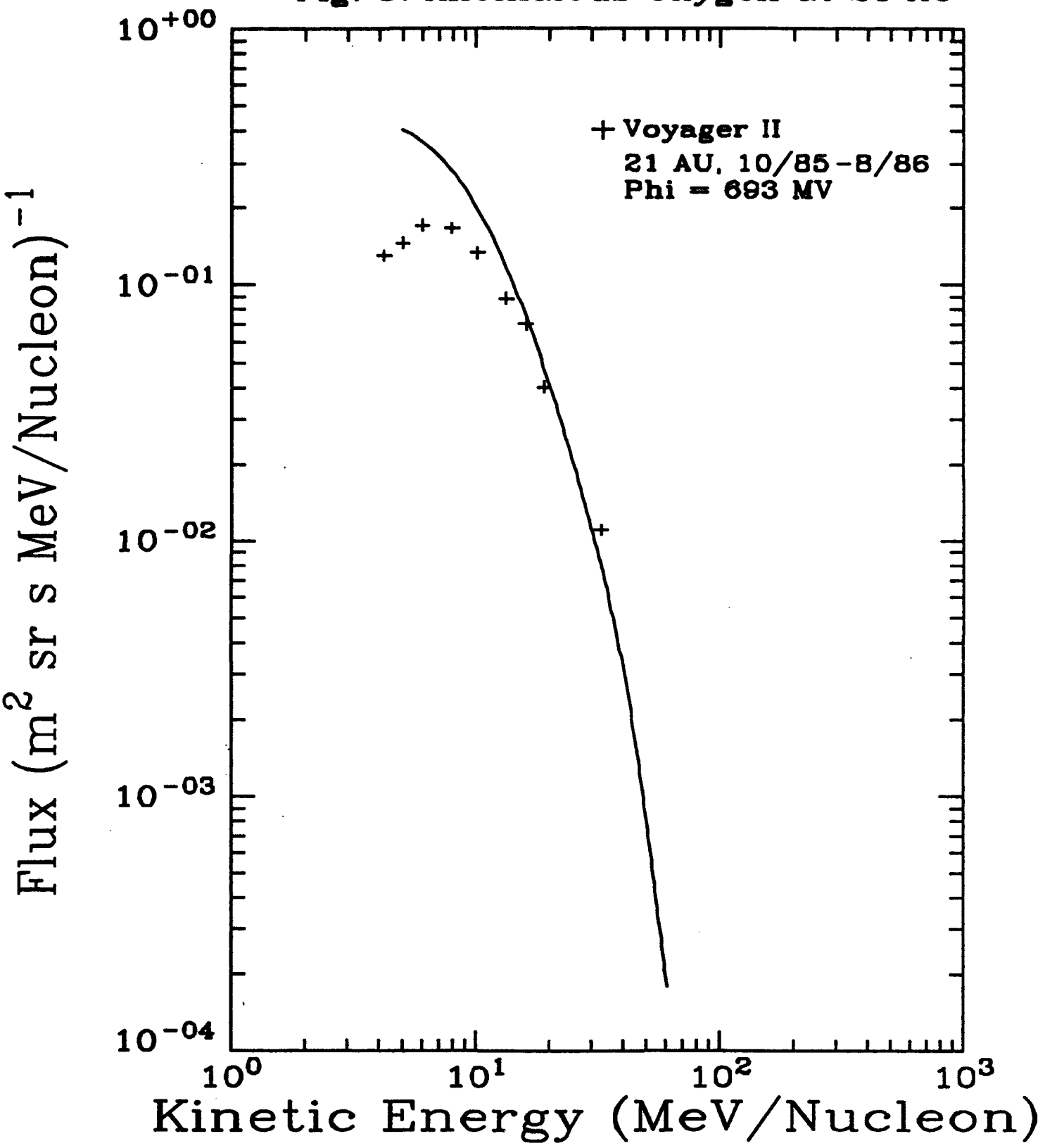

Fig. 6. Anomalous Nitrogen at 2 AU

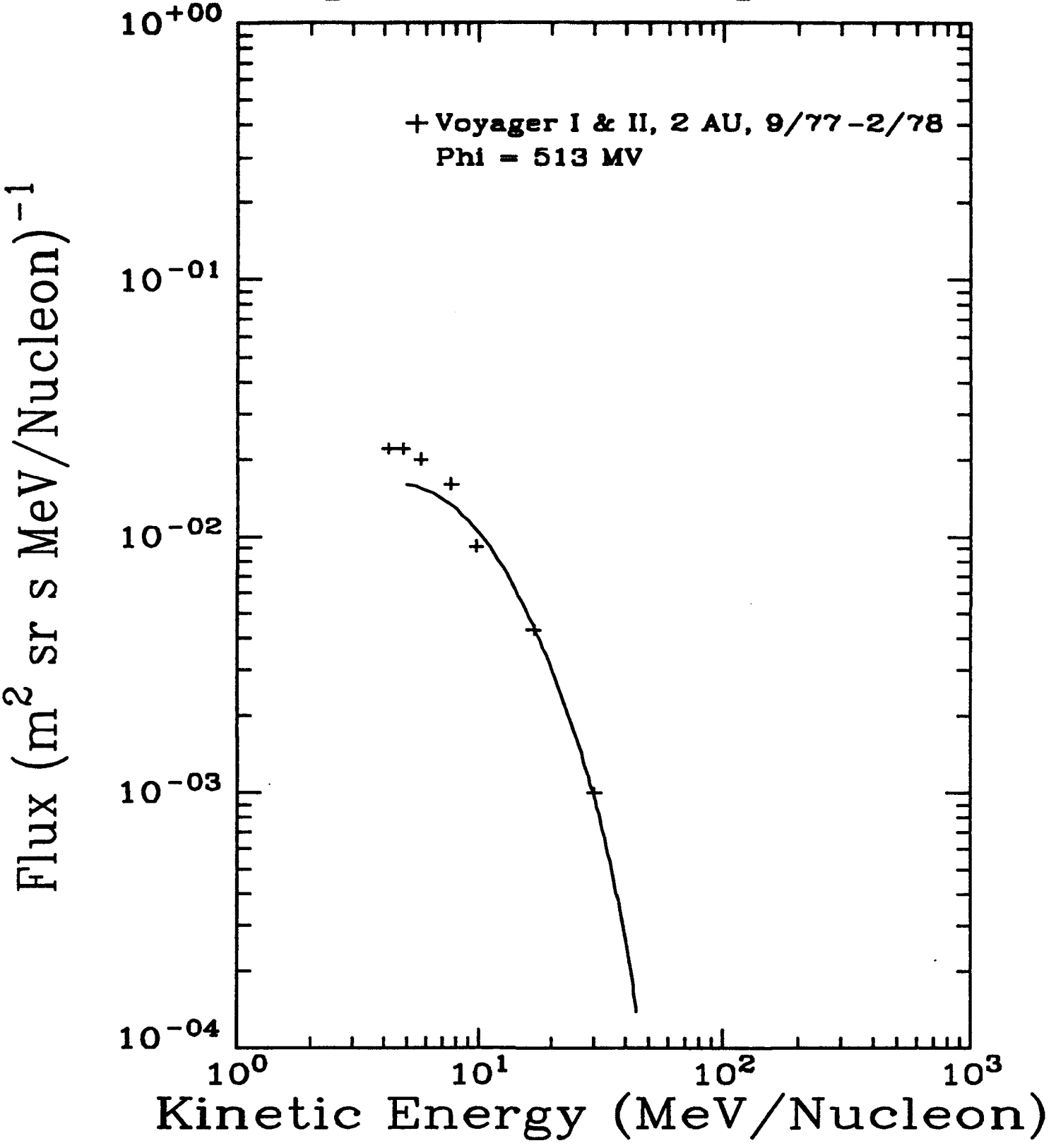

Fig. 7. Anomalous Nitrogen at 21 AU

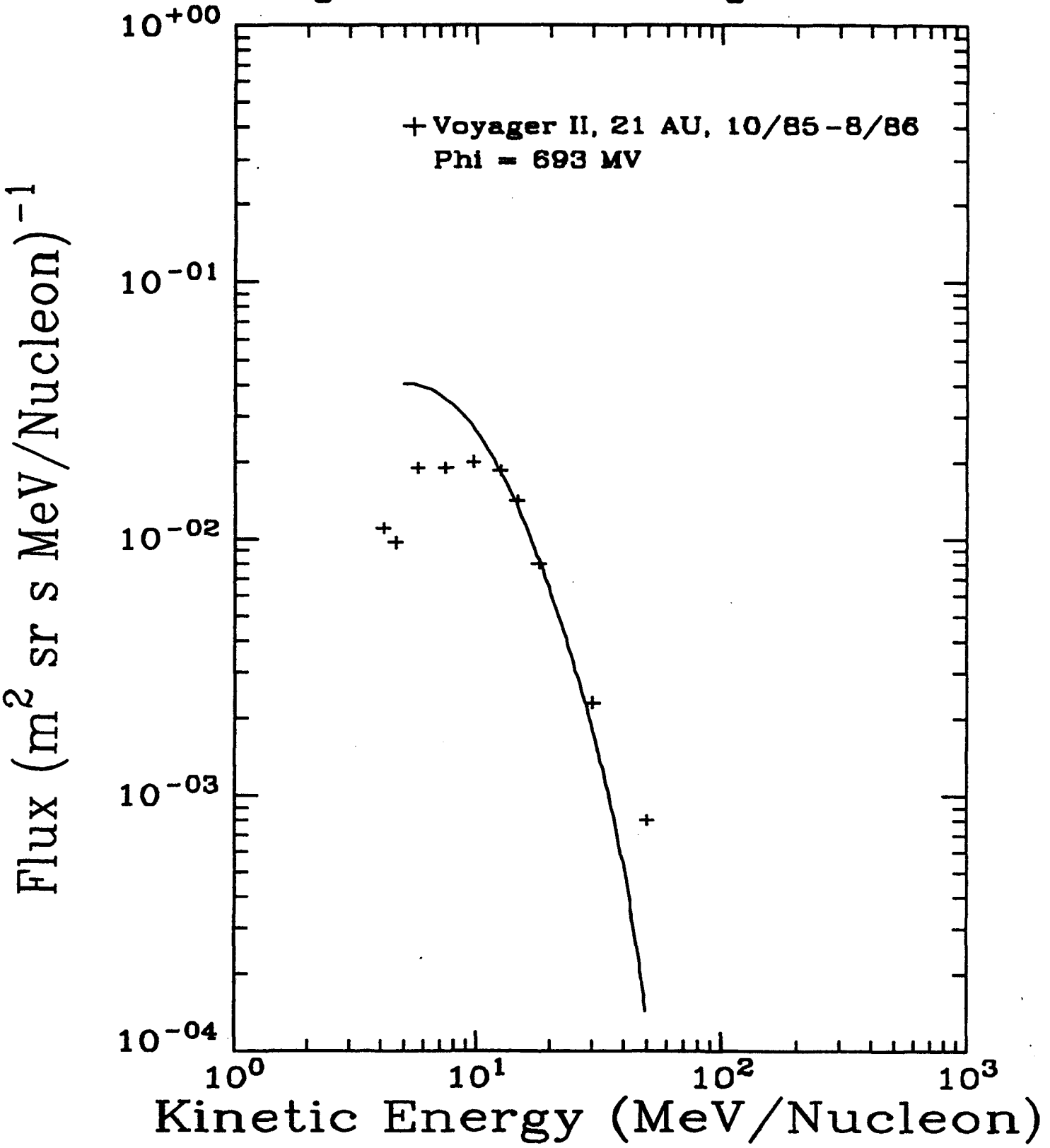

Fig. 8. Anomalous Neon at 2 AU

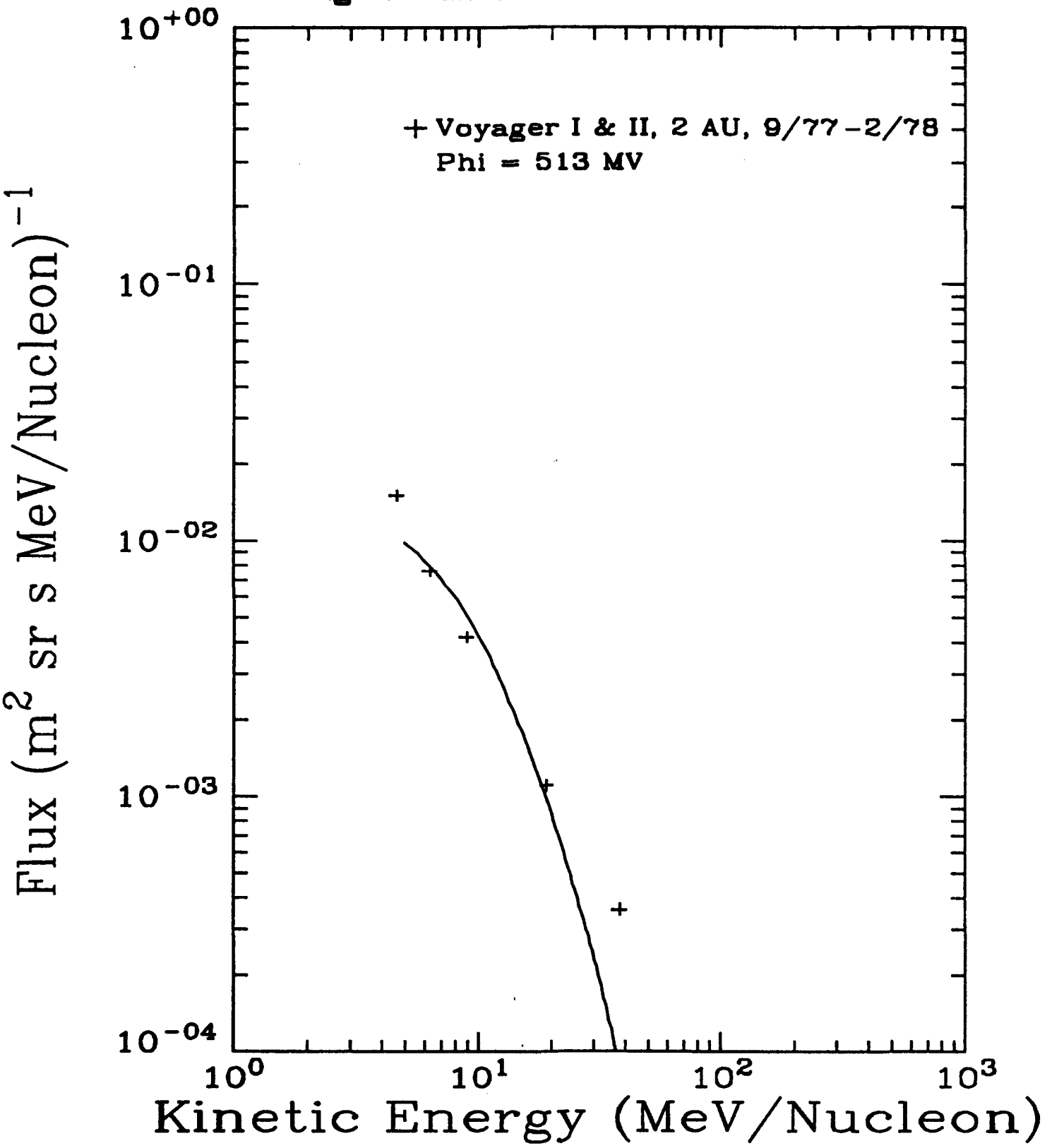

Fig. 9. Anomalous Neon at 21 AU

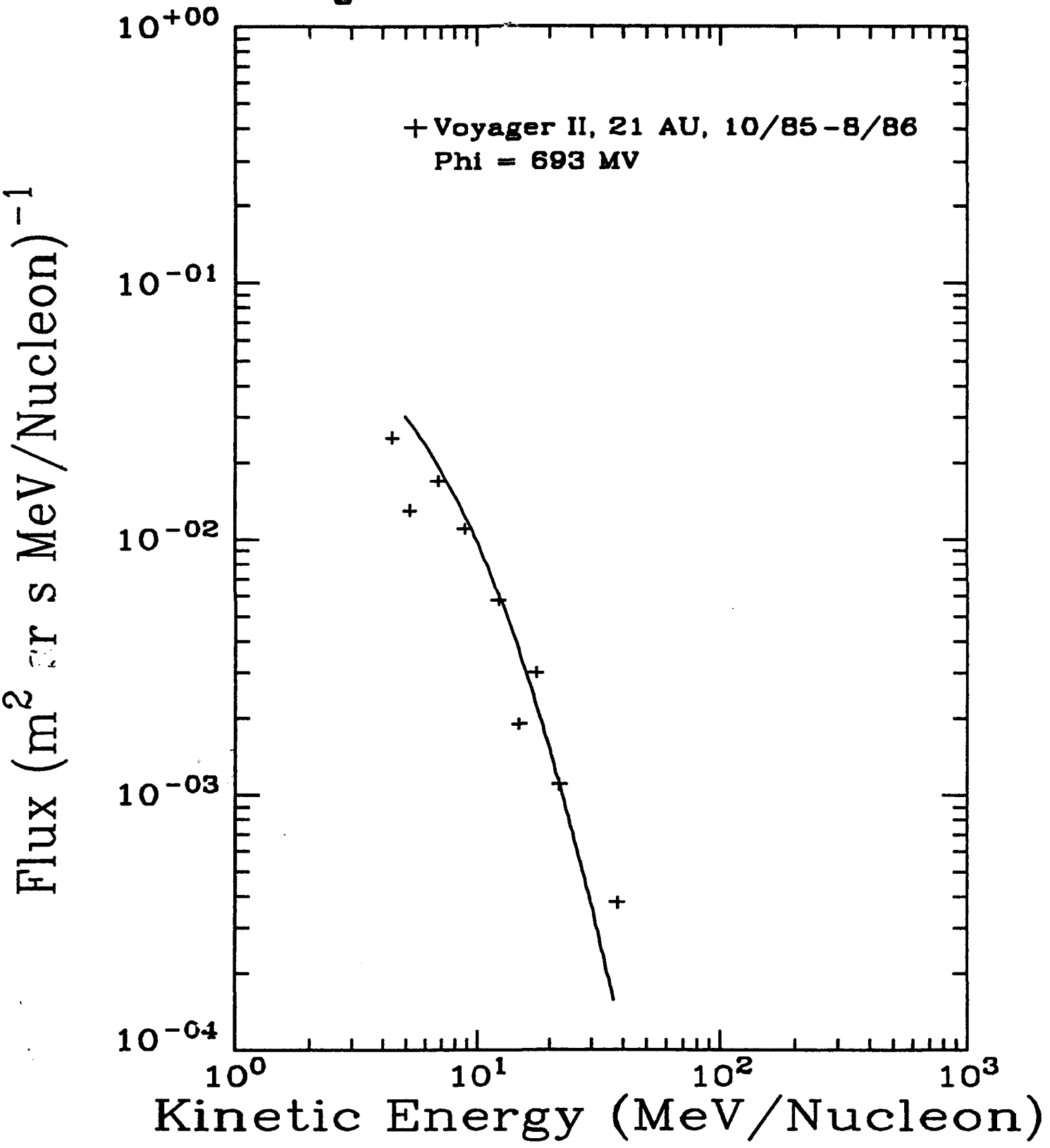

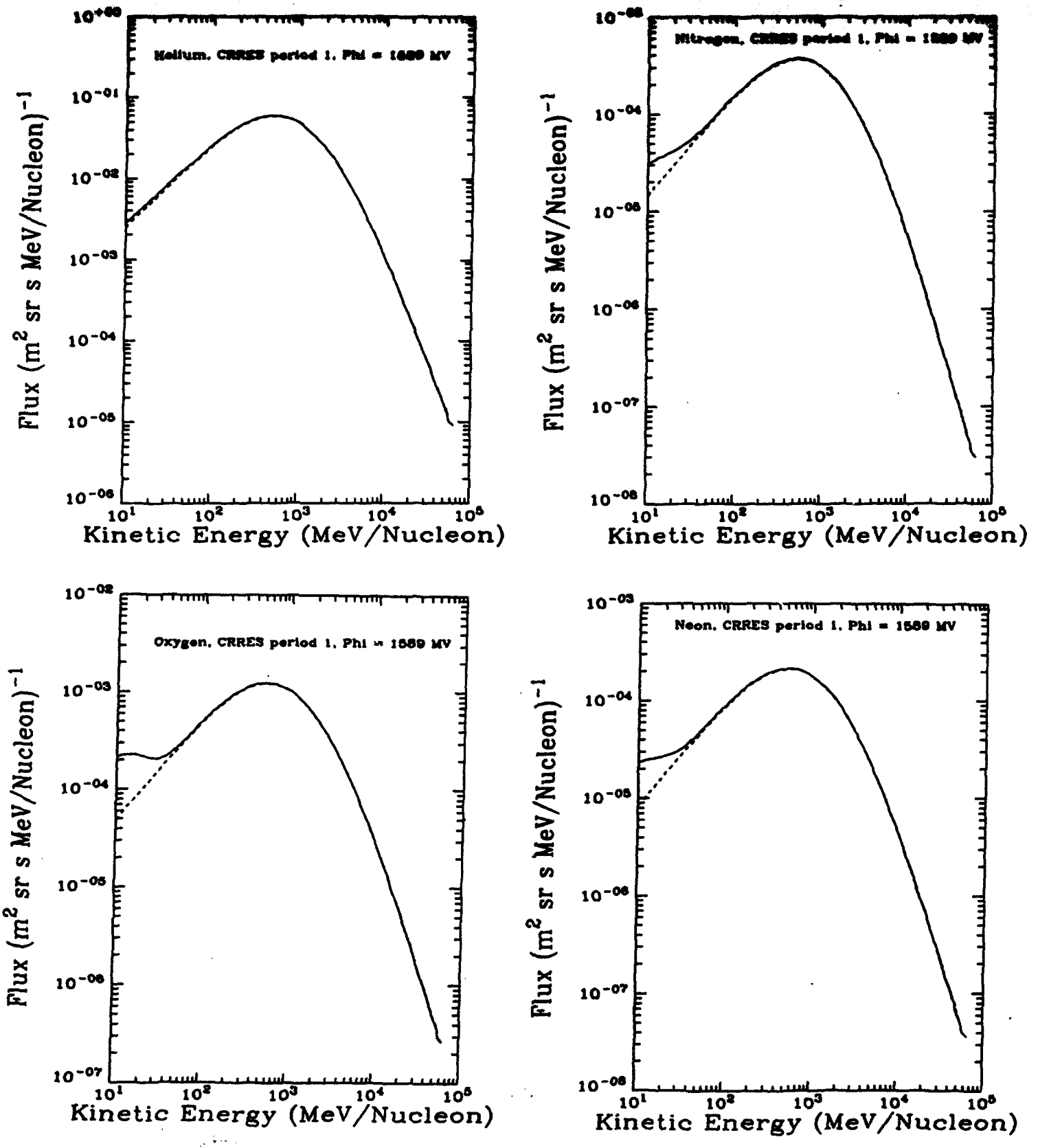

Figure 10. Calculated spectra at $\phi = 1589$ MV for He, N, O and Ne without (dashed) and with (solid) the Anomalous Component.

III. Solar Modulation Level:

In the previous report we described an evaluation of the level of solar modulation -- the ϕ parameter -- based upon the IMP-8 helium flux. That evaluation suffered from the presence of anomalous helium in the data, which was not included in the calculations. Employing the final GCR helium spectra and the anomalous helium component, described above, we have re-done the analysis. The result is shown in Figure 11, extending from late 1973 through early 1993, the full extent of the available data. The points represent measurements of ϕ made by other groups and extracted from the literature or from private communications. Now, the agreement is excellent! We believe that this comparison fully validates the solar modulation analysis and lends confidence to the use of the derived ϕ parameter in the interpretation of the data.

One of our objectives from the study of the radiation environment in Geospace has been to use the available data and the models to predict the environment that will be encountered by spacecraft. We can proceed toward that goal for the GCR plus AC if we can predict the modulation parameter ϕ (MV). In order to predict future levels of modulation, the assumption was made that the modulation level will be periodic, following the 22-year solar cycle as discussed in the previous report. The values of ϕ for the interval January 1970 through May 1971 are, therefore, assumed to reflect the values from January 1992 through May 1993. Likewise, ϕ from November 1995 through December 2010 can be obtained from the corresponding values for November 1973 (when the IMP-8 helium data began) through December 1988. Most of the 40 year interval 1970-2010 can thus be filled in using the helium-based phi-versus-time profile in Figure 11.

In order to avoid predicting exactly the same transient features seen in the phi-versus-time plot, the set of monthly average ϕ values from 1973-93 was smoothed using a Fast Fourier Transform method, and the smoothed set of values was then translated 22 years into the past and 22 years into the future to provide estimated monthly average values. Figure 12 (top) shows these intervals, together with the established values from 1973-93. As is seen in the figure, there remain two gaps of identical length, from June 1971 through October 1973 and from June 1993 through October 1995, reflecting the fact that the IMP-8 data available at present fall 29 months short of spanning a full 22-year solar cycle.

As we have shown previously, there is a good correlation between the modulation level and the Climax (or any other) neutron monitor counting rate, for which data exist back to the 1950's. Therefore, we used the neutron monitor for the interval 6/71-10/73 as a guide in filling the gap. We assume that the overall qualitative behavior of the neutron monitor and the modulation will be similar over any time interval not chosen too short. Even over spans of months, there are changes in neutron monitor rate that are not immediately mirrored in the helium fluxes, and vice versa. Therefore, the neutron monitor information was used only as a check to help ensure that the ϕ values estimated to fill the gaps do not fail to reflect any major trends. The neutron monitor data was smoothed using the same method mentioned previously, so that just the qualitative trend of the neutron count rate can be seen. Monthly values of the modulation level for 6/71-10/73 and 6/93-10/95 were then fitted into the gaps by hand, attempting more or less to reproduce the trend of the neutron monitor data and avoid any discontinuities in the modulation level at either end of the gaps.

The resulting total set of monthly average levels of modulation for the entire interval 1970-2010, with both remaining gaps filled, is shown in Figure 12 (bottom). This is now the database used for calculating average values of the level of modulation over any specified time interval. The accuracy of these predictions will be checked only by future spacecraft measurements.

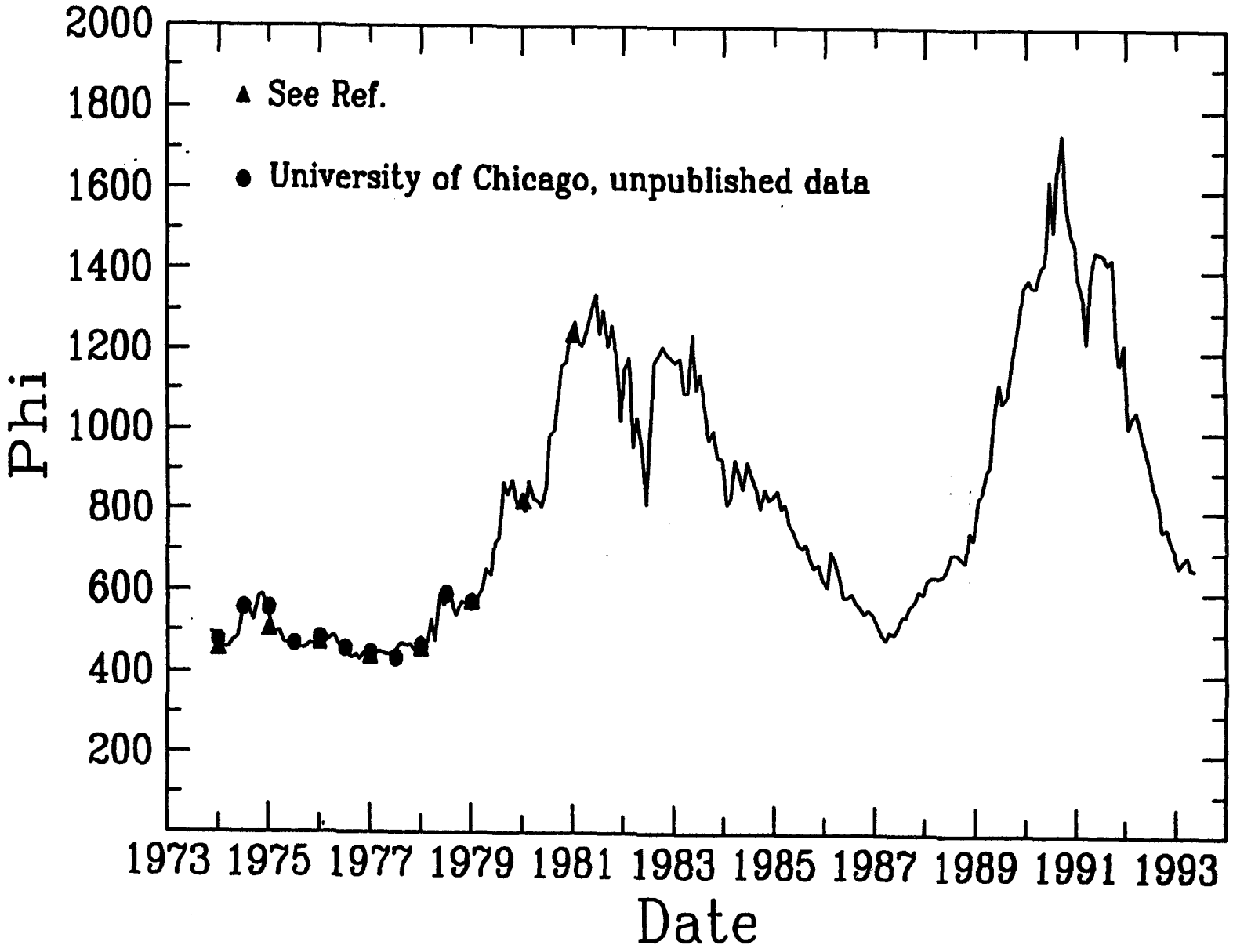

Figure 11. The derived modulation parameter ϕ(MV) as a function of time compared to measurements reported in the literature (symbols).

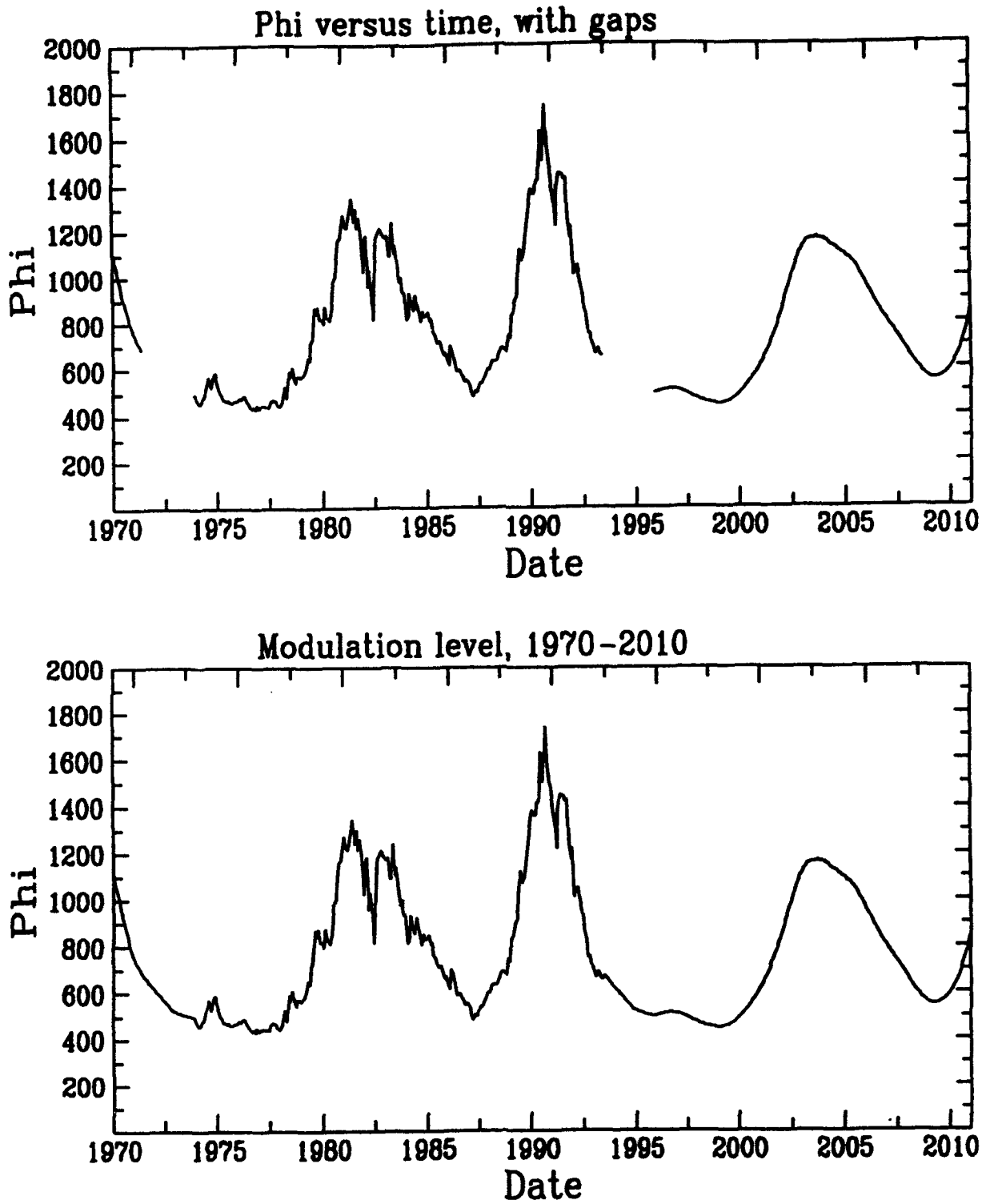

Figure 12. Modulation parameter ϕ, versus time showing the projected values based upon a 22 year solar cycle (top) and the full result, 1970 - 2010, with the gaps filled as described in the text (bottom).

IV. Particle Penetration into the Magnetosphere:

Part of our effort over the past quarter has been devoted to continuing the study of particle access into the inner regions of the magnetosphere. We have been focusing on Helium since this is a high abundance element and may be relatively straight-forward to understand. The raw data, excluding solar active periods, is shown in Figure 13 as the live-time normalized helium flux versus L shell. Direct access for Galactic Cosmic Rays is observed from high-L values with a rapid decrease in the region of L = 3-4 representing the cut-off of the GCR access. What is most interesting are the peaks at L ~2 and L ~1.3 well inside the region available to GCR events. These low-L helium are probably a "trapped" component.

The helium events are derived from the priority P2 pulse-height analyzed events after "clean-up", i.e. consistency checks, cuts on the penetration flags and angle cuts, as described in a previous report. The resulting tracks are shown for L>6 in Figure 14 where the ΔE-E matrix is plotted for both ID=7 (stopping in K1, preceding detector is D6, 1 mm thick) and ID>7 (stopping in K2-K8, preceding detector is 5 mm thick). In both cases, there is excellent charge resolution with the helium well separated from the Li and heavier ions. (Note that protons are analyzed in priority P3, so are not included in this P2 analysis except for a few background events which are eliminated by the "clean-up" procedure.)

Using the trajectory system that is included in the ONR-604 instrument on CRRES, we can measure the arrival direction of each particle. Knowing the spacecraft location, attitude and spin period we can project the arrival direction onto the local magnetic field direction to determine the particle's local pitch angle, α. The result, shown in Figure 15 for the helium with $L < 2.3$, is a distribution sharply peaked near $\cos \alpha = 0$, i.e. at α values near 90° or 270°. Such a distribution is characteristic of a trapped particle population and demonstrates that the low-L events are, at least, pseudo-trapped in the magnetosphere.

This leads directly to the question of the time dependence of the intensity of this trapped component. The CRRES results are shown in Figure 16 (top) compared to the Climax neutron monitor counting rate (bottom). The Climax data give an idea of the state of the heliosphere by recording the high energy cosmic ray intensity. During the first part of the CRRES mission, the neutron monitor rate increased slowly as the solar cycle moved from solar maximum towards solar minimum. During this period the trapped helium intensity decreased by ~30%. This argues that the low-L helium (a) is not being replenished by galactic cosmic rays, and (b) is a slowly decaying population.

The cosmic ray recovery was interrupted by the major solar events of March-June 1991 including the 3/24/91 substorm which formed a "new" radiation belt, as reported from CRRES data. During this period the trapped helium continued to decrease. This shows that the helium was not injected by the 1991 SEP events as had been suggested previously. If anything, it could be argued (within the very small statistics) that some of this trapped helium was removed by the substorm. Throughout the rest of the CRRES period the trapped helium continues to be present at a reduced intensity.

The suggestion of a solar flare injection origin cannot be totally ruled out by Figure 16. Rather we can say that the 1991 flares did not provide any injection. Whether a flare such as those at the end of 1989 could have provided the particles (and we are observing the decay of this component) cannot be determined from the present dataset.

We have divided the data into two groups at orbit 585, the peak of the flare of March, 1991. The normalized L dependence for these two periods is shown in the bottom two panels of Figure 17. Note that before the March flare events at L~1.9 are dominant while after the flare (even considering the small statistics) the L~1.9 peak is almost gone. Thus, the decrease in the trapped helium rate shown in Figure 16 appears to be due almost entirely to a reduction in the peak at L~1.9. A more detailed time history will be required to investigate this effect in detail.

The distributions in Figure 17 may be the edges of a single distribution, centered upon the inner radiation belt. For this to be the case, the ONR-604 instrument would have had to be insensitive to events occurring between L~1.3 and L~1.8. This could result if the pulse-height analysis was disabled due to high detector counting rates, so that the logic circuits never received the appropriate signals for P2 analysis. To begin to look at this possibility, the top panel of Figure 17 plots the P3 counting rate as a function of L. (Note the logarithmic scale.) Above ~10^5 in this rate, we could expect problems in the logic and the inner edges of the Helium distributions correspond to rates of a few times 10^5. Thus, it is possible that what we are observing is in fact a region of trapped high energy helium co-located with the inner proton radiation belt but slightly broader in L than the proton belt.

Clearly additional analysis will be required to verify these tentative conclusions. This will be one of the thrusts of our work for the next quarter.

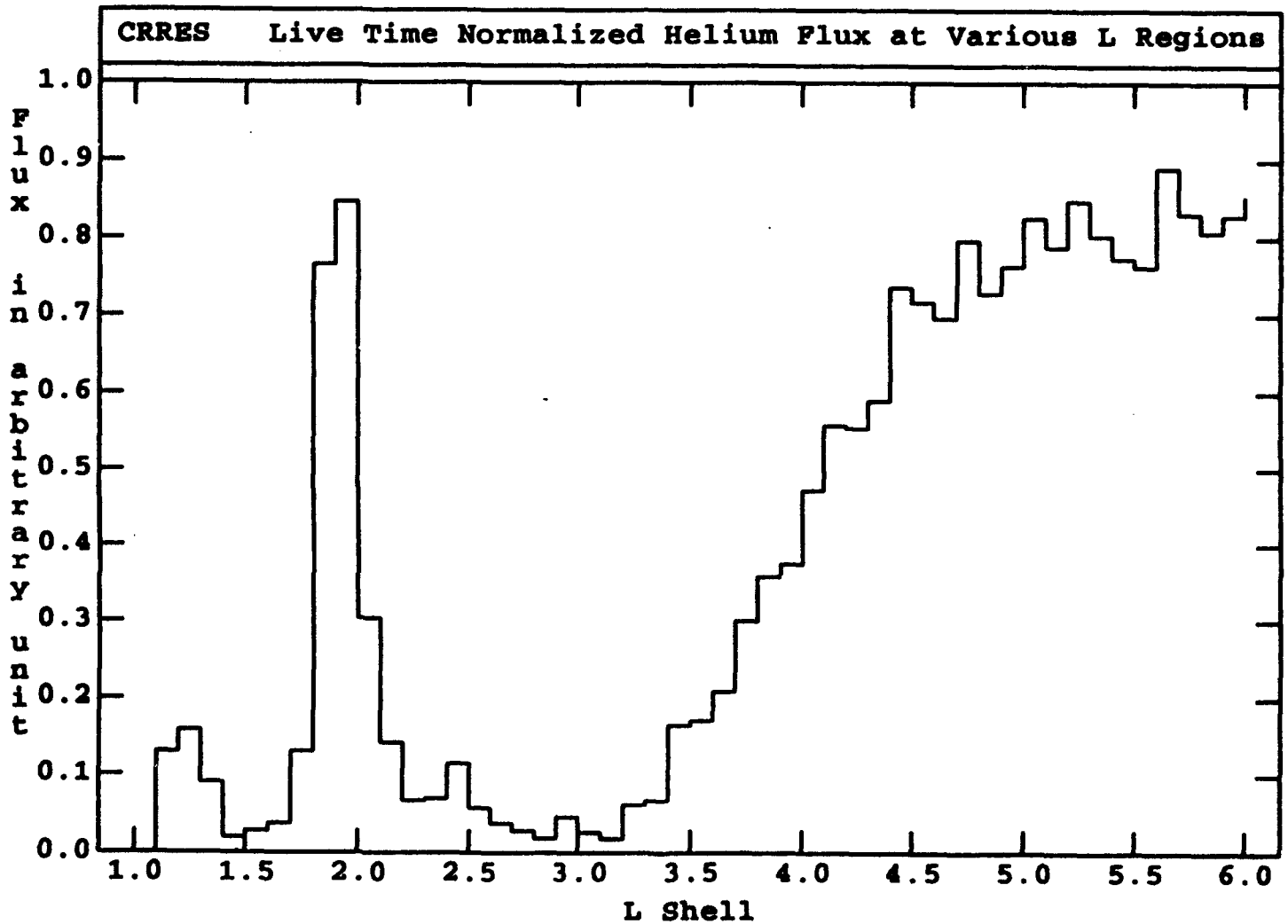

Figure 13. The normalized L distribution of quiet-time Helium events.

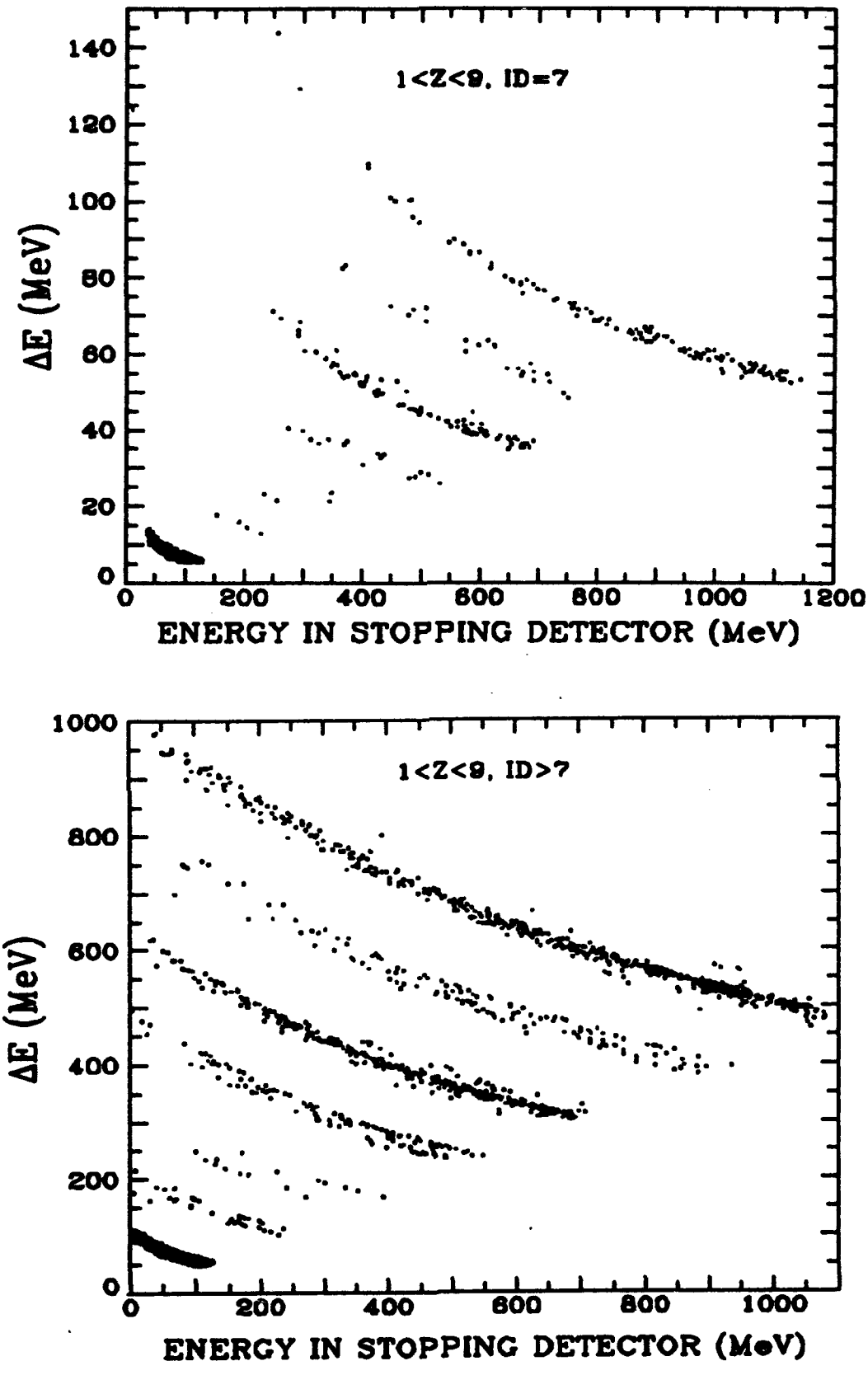

Figure 14. P2 data in ΔE-E format for He-O from quiet-times. Results are shown for ID=7 (top) and ID>7 (bottom) for orbital intervals with L>6.

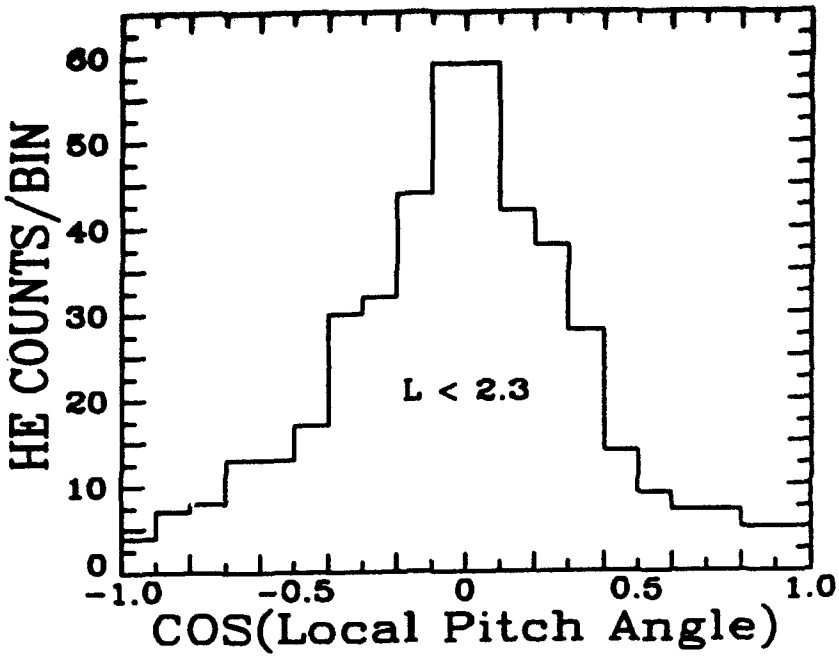

Figure 15. Pitch-angle distribution for the Helium at L<2.3.

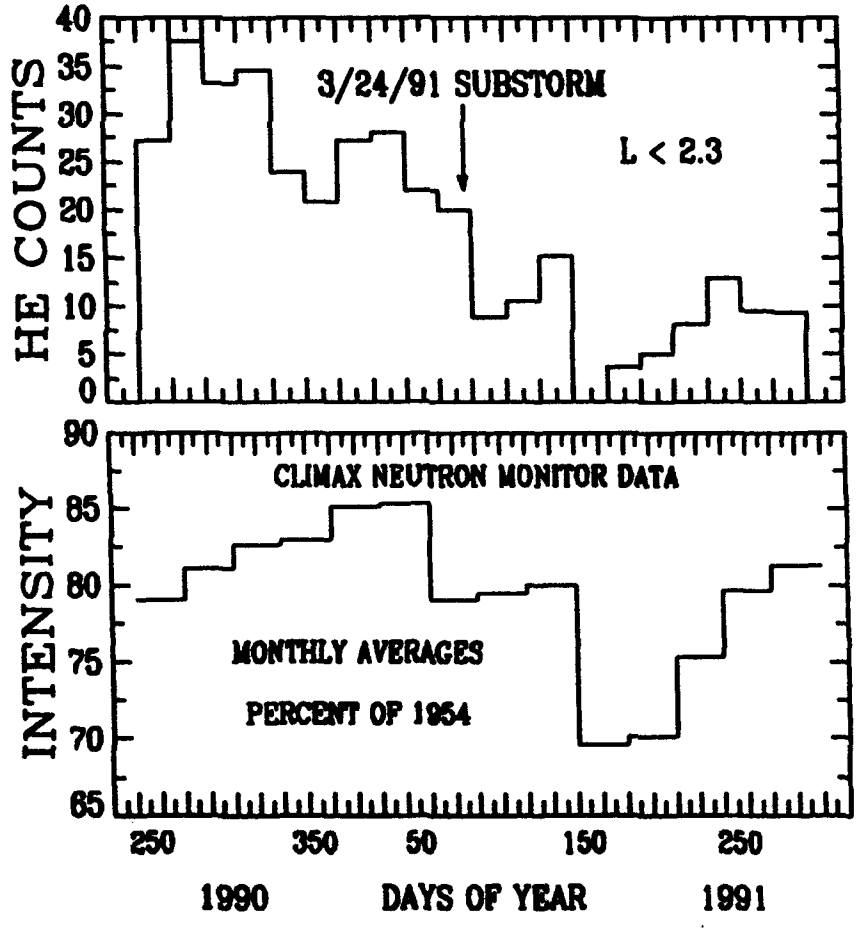

Figure 16. Time dependence of the Helium rate compared to the Climax neutron monitor rate for the period of the CRRES mission.

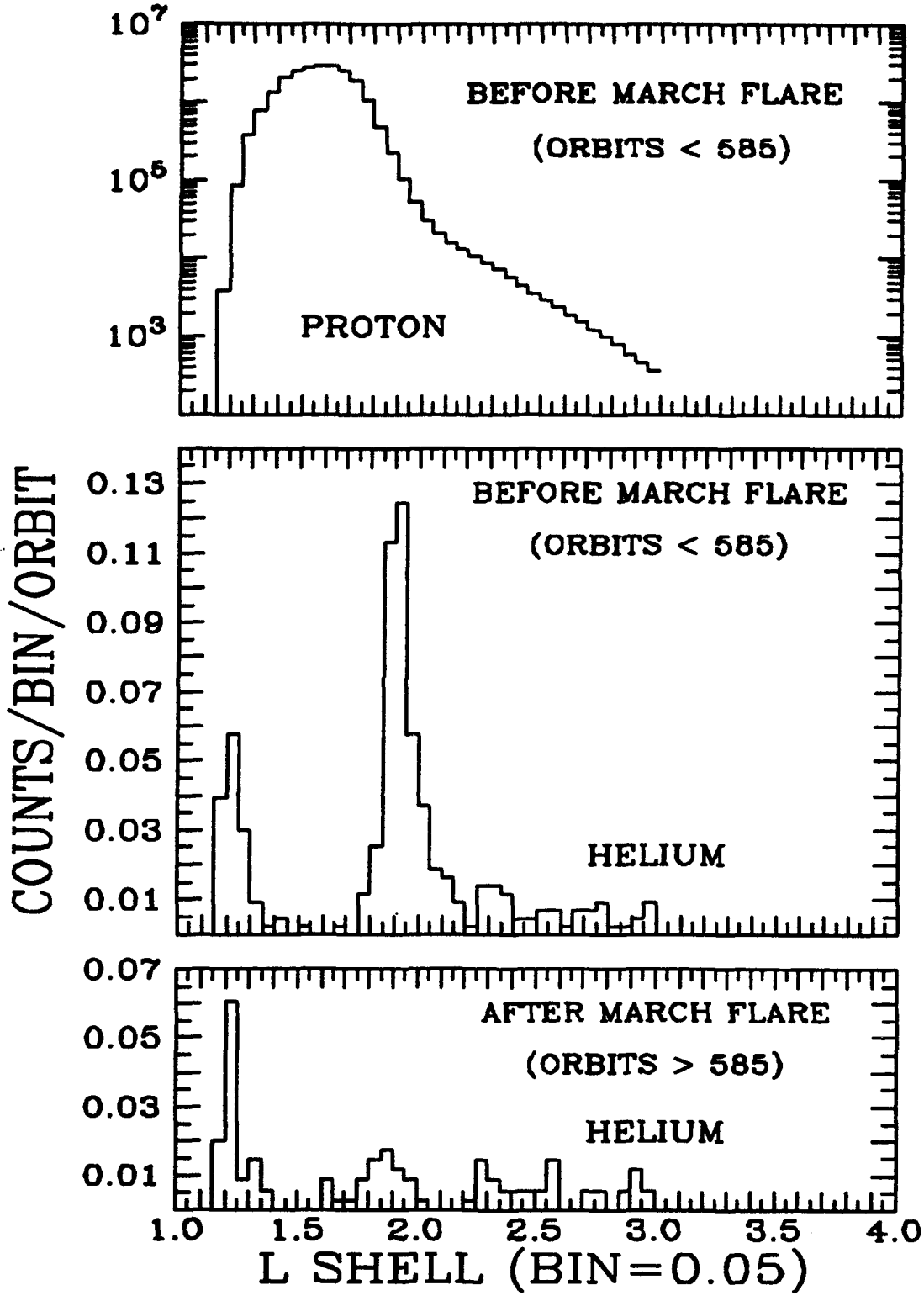

Figure 17. L dependence of the P3 (proton) counting rate (top) compared to the trapped helium distribution before (middle) and after (bottom) the peak of the flare of March, 91 (orbit 585).